EPJ manuscript No.
(will be inserted by the editor)

A numerical study of the formation of magnetisation plateaus in quasi one-dimensional spin-1/2 Heisenberg models

R.M. Wießner, A. Fledderjohann, K.-H. Mütter, and M. Karbach

Physics Department, University of Wuppertal, D-42097 Wuppertal, Germany

February 1, 2008

Abstract. We study the magnetisation process of the one dimensional spin-1/2 antiferromagnetic Heisenberg model with modulated couplings over $j = 1, 2, 3$ sites. It turns out that the evolution of magnetisation plateaus depends on j and on the wave number q of the modulation according to the rule of Oshikawa *et al.*. A mapping of two- and three-leg zig-zag ladders on one dimensional systems with modulated couplings yields predictions for the occurence of magnetization plateaus. The latter are tested by numerical computations with the DMRG algorithm.

PACS. 75.10b, 75.10Jm, 75.45+j

1 Introduction

The formation of gaps and plateaus in the magnetisation process of one-dimensional (1D) spin-1/2 antiferromagnetic Heisenberg models has been studied intensively during the last years [1,2,3,4,5,6,7,8,9,10].

Oshikawa, Yamanaka and Affleck [1] pointed out the crucial role which play the *soft modes*, predicted by the Lieb-Schultz-Mattis (LSM) construction [11]. For example in the case of the 1D spin-1/2 Hamiltonian with nearest neighbour couplings and a homogeneous external field B:

$$\mathbf{H}(B) \equiv \mathbf{H}_1 - B\mathbf{S}_3(0), \tag{1.1}$$

$$\mathbf{H}_j \equiv 2\sum_{l=1}^{N} \mathbf{S}_l \cdot \mathbf{S}_{l+j}, \quad n = 1, 2, \dots, \tag{1.2}$$

$$\mathbf{S}_a(q) \equiv \sum_{l=1}^{N} e^{ilq} S_l^a, \quad a = 1, 2, 3, \tag{1.3}$$

the ground state $|0\rangle$ has momentum $p_s = 0, \pi$ and total spin $S_T^3 = S_T = NM(B)$, where $M(B)$ is the magnetisation.

The LSM construction [11,12] leads to gap-less excited states $|k\rangle$:

$$|k\rangle = \mathbf{U}^k|0\rangle, \quad \mathbf{U} \equiv \exp\left(-i\frac{2\pi}{N}\sum_{l=1}^{N} lS_l^3\right), \tag{1.4}$$

with momenta

$$p_k = p_s + kq_3(M), \quad q_3(M) \equiv \pi(1-2M), \tag{1.5}$$

e.g. for $M = 1/4$ one finds a four fold degeneracy of the ground state with momenta $p_k = p_s + k\pi/2$, $k = 0, 1, 2, 3$. The magnetisation curve for the system (1.1) has no plateaus. The latter appear, if translational invariance is broken, by adding to (1.1) a periodic perturbation with wave vector q, e.g.:

$$\bar{\mathbf{D}}_j(q) \equiv \frac{1}{2}\left[\mathbf{D}_j(q) + \mathbf{D}_j(-q)\right], \tag{1.6}$$

$$\mathbf{D}_j(q) \equiv 2\sum_{l=1}^{N} e^{iql}\mathbf{S}_l \cdot \mathbf{S}_{l+j}, \quad j = 1, 2, \dots. \tag{1.7}$$

So far the case $j = 1$ has been studied in detail [10]. A pronounced plateau has been found in the magnetisation curve if the period ($q/\pi = 1/2, 1/6, 1/3$) coincides with the *first* soft mode ($k = 1$), $q = q_3(M) = \pi(1-2M)$, i.e. a perturbation $\bar{\mathbf{D}}_1(\pi/2)$ generates a plateau at $M = 1/4$. However, adding to (1.1) a perturbation $\bar{\mathbf{D}}_1(\pi)$ no plateau has been observed at $M = 1/4$. In the latter case the *second* soft mode at $q = \pi$ ($k = 2$) coincides with the period of the perturbation. Therefore, the question arises, why certain possibilities for the formation of plateaus, which are allowed according to the quantisation rule of Oshikawa *et al.* [1], are nevertheless not realized with a given perturbation. One possible answer to this question has been given in Ref. [10]: The efficiency of the mechanism to generate a plateau, by means of a periodic perturbation $\mathbf{D}_1(q)$, crucially depends on the magnitude of transition matrix elements $\langle n|\mathbf{D}_1(q)|0\rangle$ from the ground state $|0\rangle$ to the low-lying excited states $|n\rangle$. For example for $M = 1/4$ the transition matrix elements $\langle n|\mathbf{D}_1(\pi/2)|0\rangle$ turn out to be large whereas $\langle n|\mathbf{D}_1(\pi)|0\rangle$ are small. The effect can be seen directly in the static dimer-dimer structure factor $\langle 0|\mathbf{D}_1(q)\mathbf{D}_1(-q)|0\rangle$ for $M = 1/4$ (cf. Fig. 4 in Ref. [10]), which has a pronounced peak at $q = \pi/2$ but no peak for

$q = \pi$. Of course all these statements only hold for the nearest neighbour Hamiltonian (1.1).

Indeed, Totsuka [3] has recently observed a magnetisation plateau at $M = 1/4$, which was created by adding to the Hamiltonian (1.1) a perturbation $\bar{\mathbf{D}}_1(\pi)$ and a strong next-to-nearest neighbour coupling.

In this paper we show that the magnetisation plateau at $M = 1/4$ can be realized as well with perturbations of period $q = \pi$, if the perturbation operator is chosen properly. We will discuss in detail the situation with the operator $\bar{\mathbf{D}}_2(q)$ defined in (1.6). Note, that both operators $\bar{\mathbf{D}}_1(q)$ and $\bar{\mathbf{D}}_2(q)$ have the same momentum- and spin-symmetry properties; they change the momentum by $\pm q$ and do not change the total spin. They only differ in the isotropic spin-spin couplings, which extend over nearest neighbours in $\bar{\mathbf{D}}_1(q)$ and over next-nearest-neighbours in $\bar{\mathbf{D}}_2(q)$.

In Sec. 2 we compare the static structure factors, $S_j \sim \langle 0|\mathbf{D}_j(q)\mathbf{D}_j(-q)|0\rangle,\ j = 1, 2$, in the presence of a magnetic field with magnetisation $M = 1/4$. In Sec. 3 we study the magnetisation plateaus induced by the periodic perturbation $\bar{\mathbf{D}}_2(q)$ at $q = \pi$.

The zig zag ladder with two (and three) legs – recently investigated in Ref. [13] – can be mapped on a 1D system with translation invariant coupling over one and two (three) lattice spacings and a translation invariance breaking coupling of the type $\bar{\mathbf{D}}_2(q)$. In Sec. 4 we analyse the sequence of magnetisation plateaus, which appears in the zig-zag ladder system.

It should finally be added that the operators and Hamiltonians refer to periodic boundary-conditions in leg directions. The DMRG results given in Sec. 4, however, have been obtained using open boundary-conditions along the legs.

2 Signals of soft modes in static structure factors

In this section we discuss some properties of the static structure factors $\langle 0|\mathbf{D}_j(q)\mathbf{D}_j(-q)|0\rangle,\ j = 1, 2$, of the Hamiltonian (1.1). In order to compute static structure factors we use periodic boundary conditions and exact Lanczos diagonalizations up to $N = 24$ sites.

Soft modes, as predicted by the LSM construction, can be seen directly as zeros in the dispersion curve [10]:

$$\omega(q, M) = E(p_s + q, S + 1) - E(p_s, S), \quad M = S^z_T/N, \tag{2.1}$$

where $E(p, S)$ are the lowest energy eigenvalues with total spin $S = S_T$ and momentum p. The ground-state momentum p_s in the sector with total spin S is known to be 0 or π[14]. The zeros of (2.1) – in the limit $N \to \infty$ – appear at the soft mode momenta $q = q^{(k)}(M)$. For example, at $M = 1/4$ three zeros at $q/\pi = 0, 1/2, 1$ emerge in the dispersion curve for the Hamiltonian (1.1) (cf. Fig. 3 of Ref. [10]).

The operators $\mathbf{D}_j(q)$, $j = 1, 2$, defined in Eq. (1.7), commute with the total spin squared $\mathbf{S}^2_T$ and the dispersion curve (2.1) describes the lowest-lying excitations, which can be reached with these operators. The transition matrix element

$$\langle n|\mathbf{D}_j(q)|0\rangle, \quad j = 1, 2, \tag{2.2}$$

from the ground state $|0\rangle$ with total spin $S = S_T$ and momentum p_s to the excited states $|n\rangle$ with momentum $p = p_s + q$ enter in the corresponding static structure factor:

$$S_j(q, M) \equiv \frac{1}{N}\sum_n (1 - \delta_{n0})|\langle n|\mathbf{D}_j(q)|0\rangle|^2 \tag{2.3}$$

The signals of the soft modes in the static structure factor therefore measure the magnitude of the transition matrix elements (2.2). In Figs. 2.1(a) and 2.1(b) we compare the q-dependence of the static structure factors $S_j(q, M = 1/4)$. Indeed we observe remarkable differences. We find a

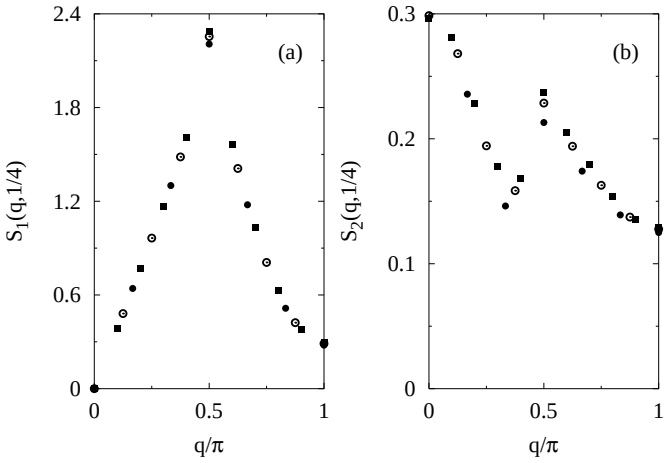

Fig. 2.1. Comparison of the q-dependence of the static structure factors (2.3) at $M = 1/4$ for the dimer operators (1.6) over nearest [(a) $j = 1$] and next-nearest-neighbour [(b) $j = 2$] couplings in a model with Hamiltonian (1.1). The different symbols belong to system sizes: $N = 20$ (■), 16(○), 12 (●).

pronounced peak in both structure factors $S_j(q, 1/4)$, $j = 1, 2$ at the soft mode $q^{(1)}(1/4) = \pi/2$. The size of the peaks, however, differ by an order of magnitude. There is no peak at the second soft mode $q^{(2)}(1/4) = \pi$. Note the different behaviour of the structure factor. For $q \to 0$: $S_1(q, 1/4)$ converges to zero whereas $S_2(q, 1/4)$ approaches a maximum $\lesssim 0.3$. This feature will play a crucial role, if we add to (1.1) a periodic perturbation $\delta \cdot \bar{\mathbf{D}}_j(\pi),\ j = 1, 2$ of strength δ. The perturbation is invariant under translations by two lattice spacings. Eigenstates of the perturbed Hamiltonian are constructed by a superposition of momentum eigenstates with $p = 0$ and $p = \pi$. The reduction of the Brioullin zone is taken into account in a

modification of the dimer operators:

$$\mathbf{D}_j^\kappa(q) \equiv 2 \sum_{l=0}^{N/2-1} e^{iq2l}\ \mathbf{S}_{2l+\kappa} \cdot \mathbf{S}_{2l+j+\kappa}, \quad \begin{cases} j = 1, 2 \\ \kappa = 0, 1. \end{cases} \tag{2.4}$$

The corresponding structure factors, defined by:

$$S_j^\kappa(q, M) \equiv \frac{1}{N} \left[\langle 0|\mathbf{D}_j^\kappa(q)\mathbf{D}_j^\kappa(-q)|0\rangle - \left|\langle 0|\mathbf{D}_j^\kappa(q)|0\rangle\right|^2 \right], \tag{2.5}$$

are symmetric under the mapping $q \to \pi - q$.

In Fig. 2.2(a) we present the static structure factor $S_1^\kappa(q, 1/4)$, $\kappa = 0, 1$ – obtained from the ground state of the Hamiltonian (1.1) with perturbation $\delta \cdot \bar{\mathbf{D}}_1(\pi)$, $\delta = 0.5$. In

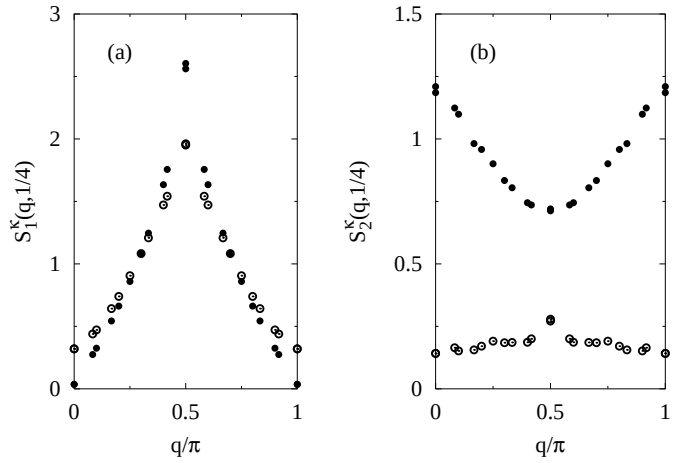

Fig. 2.2. Comparison of the q-dependence of the static structure factor (2.5) at $M = 1/4$ for the dimer operators (2.4) in a model with Hamiltonian (1.1) and perturbation $\delta \cdot \mathbf{D}_j^\kappa(\pi)$, $\kappa = 0(\bullet), 1(\circ)$; $j = 1(\text{a}), 2(\text{b})$. The perturbation strength is $\delta = 0.5$, the system sizes are $N = 20, 24$.

both structure factors we only find a peak at $q = \pi/2$ but no peak at $q = 0, \pi$. The situation for the static structure factors $S_2^\kappa(q, 1/4)$, $\kappa = 0, 1$ is shown in Fig. 2.2(b). Here the ground state has been computed for Hamiltonian (1.1) with a perturbation $\delta \cdot \bar{\mathbf{D}}_2(\pi)$, $\delta = 0.5$. Note the different behaviour of the two structure factors $S_2^\kappa(q, 1/4)$, $\kappa = 0, 1$. $S_2^1(q, 1/4)$ has its maximum at $q = 0, \pi$, whereas $S_2^2(q, 1/4)$ has a maximum at $q = \pi/2$. We therefore expect that the operator $\bar{\mathbf{D}}_2(\pi)$ generates a plateau at $M = 1/4$, whereas the operator $\bar{\mathbf{D}}_1(\pi)$ does not.

3 Magnetisation plateaus induced by periodic perturbations

Periodic perturbations of the type $\bar{\mathbf{D}}_j(q)$ – added to the nearest neighbour Hamiltonian (1.1) – generate a characteristic sequence of plateaus in the magnetisation curve. We dicsuss the same Hamiltonian for which we have computed the static structure factor in Sec. 2.2. For this reason we also apply periodic boundary conditions in this section.

The possible position of the plateaus is given by the quantisation rule of Oshikawa *et al.* [1]. However, whether or not a plateau really appears, crucially depends on the type of the perturbation operator. As an example we compare in Fig. 3.1 the evolution of the magnetisation plateaus generated by the operators $\bar{\mathbf{D}}_1(\pi)$ and $\bar{\mathbf{D}}_2(\pi)$.

The magnetisation curves – generated with $\bar{\mathbf{D}}_1(\pi)$, cf. Fig. 3.1 column (a) – show a plateau at $M = 0$, rapidly increasing with the strength δ of the perturbation. This is the well known gap induced by dimerisation. There is no plateau at $M = 1/4$ in the whole δ range ($0 < \delta \lesssim 0.7$).

In contrast the magnetisation curves – generated with $\bar{\mathbf{D}}_2(\pi)$, [cf. Fig. 3.1 column (b)] – have no plateau at $M = 0$. For $\delta \gtrsim 0.4$ a plateau appears at $M = 1/4$. A finite-size analysis of the plateau width yields the δ-evolution shown in Fig. 3.2.

Note in particular, the drastic change in the plateau width at $\delta = 0.7$. This feature is associated with a change in the ground-state quantum numbers in the fixed S_T^z-sectors. For $\delta < 1/2$ all ground states ($0 \le M \le 1/2$) have the standard momentum $0, \pi$. The first change happens in the sector $M = 1/2$–$1/N$ at $\delta = 1/2$, where the ground state is degenerate with momentum $p = 0, \pi$ and $p = \pm\pi/2$.

For larger values of δ ($\delta > 1/2$) we observe a different ground-state behaviour in the sectors with:

$$0 \le M \le M_0(\delta), \quad \text{and} \quad M_0(\delta) \le M \le 1/2. \tag{3.1}$$

In the first regime of (3.1) the ground state has still momentum $p = 0, \pi$. In contrast, in the second regime of (3.1) the ground-state momentum alternates between $p = 0, \pi$ and $p = \pm\pi/2$. The magnetisation $M_0(\delta)$, which separates the two regimes passes the plateau $M = 1/4$ exactly at $\delta = 0.7$.

The plateau structures in the magnetization curves of chains with periodic perturbations can be seen already on rather small systems ($N \approx 24$).

4 Magnetisation plateaus in zig-zag ladders

The magnetic properties of zig-zag ladders have been recently investigated by Cabra, Honecker and Pujol [13] by means of bosonization techniques and numerical analysis. In order to understand the appearance of plateaus in the magnetisation curve, a mapping of the ladder system onto a 1D spin chain with couplings over short range distances is useful. For *normal* spin ladders with l legs this mapping leads to couplings over nearest neighbour and to couplings over l lattice sites [9]. The couplings over l lattice sites appear along the legs, whereas nearest neighbour couplings form the rungs of the ladder. At the endpoints of the rungs nearest neighbour bonds have to vanish to avoid the appearance of diagonal couplings in the ladder. A Fourier analysis of the translation invariance breaking terms:

$$\sum_q \delta_q \bar{D}_1(q), \tag{4.1}$$

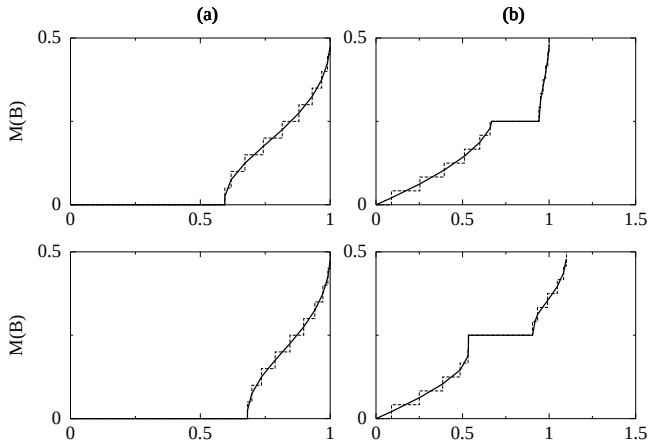

Fig. 3.1. Comparison of the plateau evolution in the magnetisation curves of a model with Hamiltonian (1.1) and perturbation $\delta \cdot \bar{\mathbf{D}}_j(\pi), j = 1(a), 2(b)$, $\delta = 0.5, 0.6$ (from top to bottom). The solid lines represent the midpoint magnetisation curves, together with extrapolated values of the upper and lower critical field B^U and B^L, respectively, deduced from system sizes $N = 8, 12, \ldots, 24$.

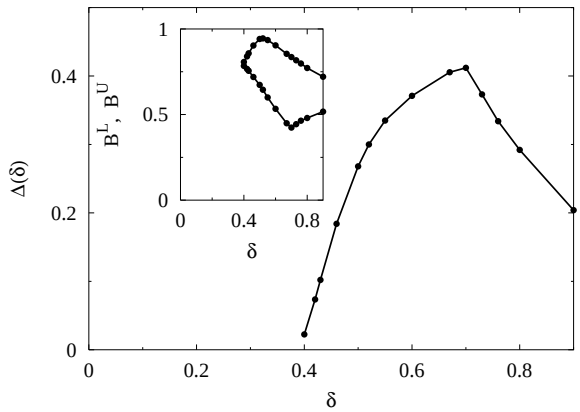

Fig. 3.2. The δ-evolution of the $M = 1/4$ plateau width $\Delta(\delta) = B^U - B^L$ in a model with Hamiltonian (1.1) and a perturbation $\delta \cdot \bar{\mathbf{D}}_2(\pi)$, deduced from system sizes $N = 12, 16, 20, 24$.

leads to a prediction of magnetisation plateaus at:

$$M = M_l^Z \equiv \frac{1}{2} - \frac{Z}{l}, \tag{4.2}$$

where Z is integer and runs over the sequence

$$Z = \begin{cases} 1, 2, 3, \ldots, l/2 & : l \text{ even} \\ 1, 2, 3, \ldots, (l-1)/2 & : l \text{ odd.} \end{cases} \tag{4.3}$$

The prediction is based on the assumption that a plateau only appears if one of the wave vectors q in the Fourier analysis (4.1) of the perturbation coincides with the *first* soft mode ($k = 1$).

In the following subsections we consider different realizations of zig-zag spin ladders, which have been discussed recently by several authors [13,15,16]. We map those systems to 1D systems with appropriate couplings over $j = 1, 2, 3$ neighbours. For some of the following systems we expect more than one plateau in the magnetization curve, therfore we use in this section DMRG calculations, which also means we apply open boundary conditions, to get a finer resolution, i.e. more steps in the finite-size magnetization curves.

4.1 The two-leg zig-zag ladder

The mapping of the two leg zig-zag ladder onto a 1D system with short range couplings is shown in Fig. 4.1. The

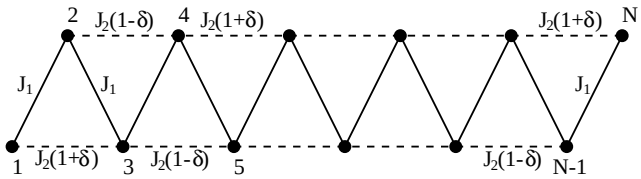

Fig. 4.1. Mapping of the two-leg zig-zag ladder onto a 1D system with Hamiltonian (4.4). The solid lines represent the nearest neighbour interactions with coupling J_1 and the dashed lines the next-nearest-neighbour interactions with couplings $J_2(1 \pm \delta)$.

Hamiltonian can be written as:

$$\mathbf{H} = J_1 \mathbf{H}_1 + J_2(1+\delta)\mathbf{H}_{+\delta} + J_2(1-\delta)\mathbf{H}_{-\delta}, \tag{4.4}$$

$$\mathbf{H}_{\pm\delta} \equiv 2 \sum_{l=1}^{N} \left[\mathbf{S}_{4l} \cdot \mathbf{S}_{4l\pm2} + \mathbf{S}_{4l+1} \cdot \mathbf{S}_{4l\pm2+1} \right]. \tag{4.5}$$

The Fourier analysis (4.1) of the translation invariance breaking terms yields in this case:

$$\mathbf{H} = \sum_{j=1,2} J_j \mathbf{H}_j + \delta J_2 \sqrt{8} \sum_{l=1}^{N} \cos\left(\frac{\pi l}{2} - \frac{\pi}{4}\right) \mathbf{S}_l \cdot \mathbf{S}_{l+2}. \tag{4.6}$$

Therefore we expect magnetisation plateaus, if the wave vector $q/\pi = 1/2, 3/2$ meets the first and second soft mode:

$$q = \frac{\pi}{2} \quad : \quad M_{4k}^1 = \frac{1}{2} - \frac{1}{4k}, \quad \text{for } k = 1, 2, \tag{4.7}$$

$$q = \frac{3\pi}{2} \quad : \quad M_{4k}^3 = \frac{1}{2} - \frac{3}{4k}, \quad \text{for } k = 2. \tag{4.8}$$

We have looked in particular for plateaus at $M_8^3 = 1/8$ and $M_8^1 = 3/8$ induced by the second soft mode $k = 2$. The situation at $J_1 = 1$, $J_2 = 2$ and $\delta = 0.6, 0.8, 1.0$ is shown in Fig. 4.2, where the emergence of a plateau at $M = 1/8$ is visible. The effect disappears if we change the ratio $\alpha = J_1/J_2$ in both directions $\alpha < 1/2$ and $\alpha > 1/2$.

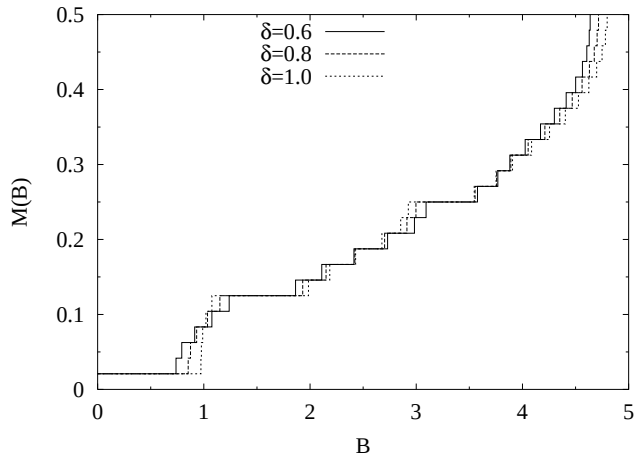

Fig. 4.2. Magnetisation curve of the two leg zig-zag ladder with Hamiltonian (4.6) with couplings: $J_1 = 1,\ J_2 = 2,\ \delta = 0.6, 0.8, 1.0$. The system size is $N = 48$.

4.2 Three-leg zig-zag ladder with periodic rung couplings

The mapping of the three-leg zig-zag ladder onto a 1D system with short range couplings is shown in Fig. 4.3. The corresponding Hamiltonian can be rewritten as:

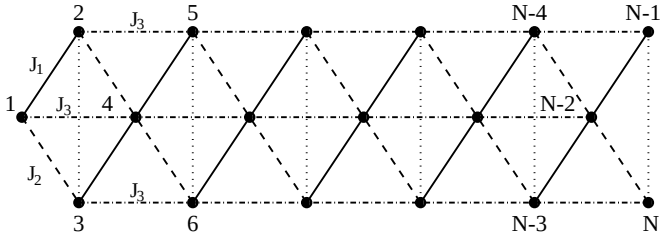

Fig. 4.3. Mapping of the three leg zig-zag ladder with periodic rung couplings onto a 1D system with Hamiltonian (4.9). The solid lines represent nearest neighbour interactions with couplings J_1, the dashed lines next-nearest-neighbour interactions with couplings J_2, and the dashed-dotted lines interactions over third neighbour interactions with couplings J_3. The dotted lines denote interactions with nearest neighbour couplings J_1, as they are enforced by periodic boundary conditions along the rungs.

$$\mathbf{H} = \sum_{j=1,3} J_j \mathbf{H}_j + \frac{2}{3} J_2 \left[\mathbf{H}_2 - 2 \sum_{l=1}^{N} \cos\left(\frac{2\pi}{3} l\right) \mathbf{S}_l \cdot \mathbf{S}_{l+2} \right]. \tag{4.9}$$

The last term on the right-hand side breaks the translation invariance of the 1D system and we therefore expect magnetisation plateaus for

$$M_3^1 = \frac{1}{6}, \quad M_6^1 = \frac{1}{3}, \quad M_9^2 = \frac{7}{18}, \tag{4.10}$$

if the wave vector $q = 2\pi/3$ meets the first ($k = 1$), second ($k = 2$) and third ($k = 3$) soft mode, respectively.

We have computed the magnetisation curves with periodic rung couplings and open boundary-conditions along the legs for the following values:

$$J_1 = \frac{3}{2} J_3, \quad J_2 = \frac{3}{2} J_3, \tag{4.11}$$

and system sizes: $N = 3 \times L,\ L = 8, 12, 16, 20, 24$. It turns out, that the midpoint extrapolation à la Bonner and Fisher [17] still shows a surprisingly large finite-size effects for the open boundary conditions. However, as can be seen from Fig. 4.4, there is still a clean signal for two plateaus at $M = 1/6$ and $M = 1/3$.

In Ref. [13], the magnetisation curve has been computed for the same set of couplings (4.11), but with different boundary-conditions along the rungs, which they call periodic boundary-conditions of type A, B or C. No plateau at all is found for type B, one plateau at $M = 1/6$ is found for type A and C. This is a first indication that the formation of plateaus critically depends on the boundary-conditions along the rungs.

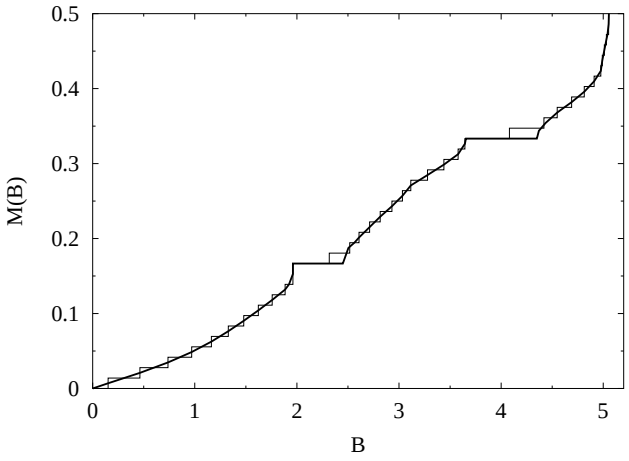

Fig. 4.4. Magnetisation curve of the three leg zig-zag ladder with periodic rung couplings and Hamiltonian (4.9) with couplings: $J_1 = 1.5,\ J_2 = 1.5$. The system size is $N = 72$. The solid line is the midpoint magnetisation curve. The behaviour at the end of the plateaus is extrapolated from data of systems $N = 24, 36, \ldots, 96$. The finite-size effects are largest in the region around the upper critical field of the plateaus.

4.3 Three-leg ladder with open rung couplings

The mapping of this system onto a 1D system with short range couplings can be seen again from Fig. 4.3. We only have to remove the dotted nearest neighbour bonds, which implement the periodic rung couplings. This changes the Hamiltonian in the following manner:

$$\mathbf{H} = \frac{2}{3} \sum_{j=1,2} J_j \left[\mathbf{H}_j - 2 \sum_{l=1}^{N} \cos\left[\frac{2\pi}{3}(l+2-j)\right] \mathbf{S}_l \cdot \mathbf{S}_{l+j} \right] + \\ + J_3 \mathbf{H}_3. \tag{4.12}$$

The two Hamiltonians (4.9) and (4.12) differ in the relative weight of the translation symmetry breaking terms.

It was found already in Ref. [13] that for the couplings (4.11) ($J_1 = 3/2,\ J_2 = 3/2,\ J_3 = 1$) the magnetisation curve for the Hamiltonian (4.12) evolves two pronounced plateaus at $M = 1/6$ and at $M = 1/3$ generated by the first and second soft mode, respectively. This is confirmed in our computation. Switching from antiferromagnetic to ferromagnetic leg coupling ($J_3 = -1$) we find spontaneous magnetisation at $M = 1/6$ whereas the plateau at $M = 1/3$ disappears (Fig. 4.5).

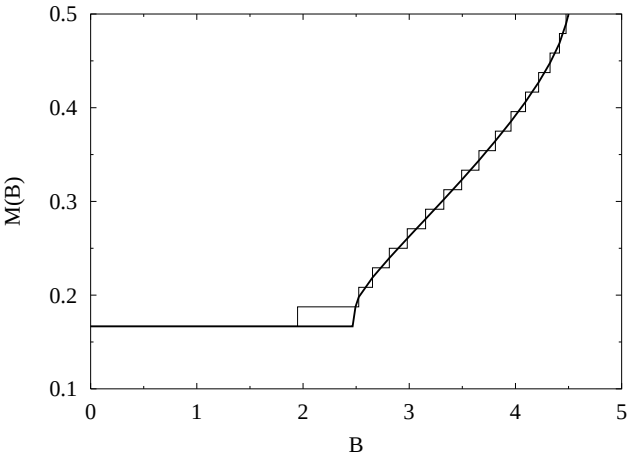

Fig. 4.5. Magnetisation curve of the three leg zig-zag ladder with open rung and leg couplings and Hamiltonian (4.12) with couplings: $J_1 = J_2 = 3/2,\ J_3 = -1$. The solid line represents the midpoint magnetisation, extrapolated from system sizes $N = 24 - 72$. The thin line is the magnetisation curve for $N = 48$.

4.4 The Kagomé like three spin ladders

This system has been studied recently in Ref. [15] for reasons which we explain below. Its couplings are defined by removing from Fig. 4.3 the middle leg and the dotted vertical lines. The mapping onto the 1D system with short range couplings then leads to the Hamiltonian:

$$\mathbf{H} = \frac{2}{3}\sum_{r=1}^{3} J_r \mathbf{H}_r - \frac{4}{3}\left(J_1 \sum_{l=1}^{N} \cos\left[\frac{2\pi}{3}(l+1)\right] \mathbf{S}_l \cdot \mathbf{S}_{l+1} + J_2 \sum_{l=1}^{N} \cos\left[\frac{2\pi}{3} l\right] \mathbf{S}_l \cdot \mathbf{S}_{l+2} + J_3 \sum_{l=1}^{N} \cos\left[\frac{2\pi}{3}(l-1)\right] \mathbf{S}_l \cdot \mathbf{S}_{l+3}, \right). \quad (4.13)$$

Equation (4.13) differs from Eq. (4.12) in the additional translation symmetry breaking term over three lattice spacings. The Kagomé like *three leg ladder* is interesting because it shares with the two dimensional Kagomé lattice the property that there is a high density of low-lying singlets. A different Kagomé like three leg ladder system has been analysed recently by Azaria *et al.* [18].

The Kagomé lattice itself seems to have a singlet-triplet gap. The authors of Ref. [15] tried to find out whether such a gap (i.e. a plateau at $M = 0$) exists as well for the Kagomé like *three spin ladder*. Extrapolation from DMRG results for systems up to 120 sites show that the system is gap-less for values of the leg spin coupling J in the interval $0.5 < 2J_3 < 1.25,\ J_1 = 1/2$. Note, that the translation invariance breaking terms in (4.13) do not generate a plateau at $M = 0$ but at $M = 1/6$ and $M = 1/3$.

Our results for fixed couplings $J_1 = J_2 = 1.0$ and increasing couplings $J_3 = 0.4, 0.6, 1.0$ are shown in Fig. 4.6. For $J_3 = 0.4$ we find spontaneous magnetisation at $M = 1/6$. This phenomenon is a consequence of the Lieb-Mattis theorem [19], as was pointed out by the authors of Ref. [15]. In condensed matter physics this phenomenon is called *ferrimagnetism*. The magnetisation curve for $J_3 = 0.6$ starts with a steep increase at $B = 0$ and reaches quickly the plateau at $M = 1/6$ for a small value of $B \approx 0.1$. Going to larger values of the coupling $J_3 = 1.0$, the slope of the magnetisation curve and the plateau width at $M = 1/6$ are reduced. At the same time, we expect the appearance of a small plateau at $M = 1/3$. Beyond this point the system jumps into the saturation magnetisation. This phenomenon is called meta-magnetism [20].

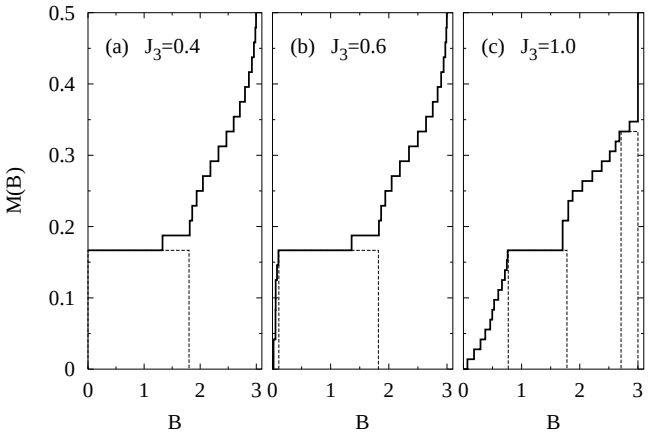

Fig. 4.6. Magnetisation curve of the Kagomé like *three spin ladder* with Hamiltonian (4.13) and couplings: $J_1 = J_2 = 1,\ J_3 = 0.4, 0.6, 1.0$. The system size is $N = 48$ for (a) and (b) and due to the larger finite-size effects $N = 72$ for (c). The dashed lines show the extrapolted postions of the plateau ends deduced from Lanczos diagonalizations with periodic boundary conditions.

We finally want to give some comments on the strong finite-size behavior of the presented DMRG calculations of magnetization curves especially appearing at the upper critical fields of the shown magnetization plateaus. Reanalyzing the 3-leg zig-zag and Kagomé like ladders

of this section for system sizes $N = 12, 18, 24$ and periodic leg boundary conditions applying standard Lanczos techniques led to a straight affirmation of the presented extrapolations. It moreover showed that the strong finite-size effects at the upper plateau edges are no genuine additional features but a simple consequence of the open leg boundary conditions used for the DMRG calculations (see e.g. plateau boundaries additionally given in Fig. 4.6). In addition, the evaluations with periodic leg boundary conditions could make clear the existence of an additional plateau ($m = 1/3$) for the Kagomé like 3-leg ladder shown in Fig. 4.6 (c), i.e. $J_3 = 1.0$. Again, at the upper critical field strong finite-size corrections hinder the identification of the $m = 1/3$ plateau on the basis of the shown DMRG results. For the two other cases –$J_3 = 0.4$, 0.6– additional plateaus could be excluded. It remains to be summarized that evaluations with both types of leg boundary conditions agree –if possible to obtain– in the thermodynamic limits of the considered quantities. Periodic boundary conditions, however, show much smaller and more controlled behavior of finite-size effects while the open boundary conditions require considerably larger system sizes for an equal quality of extrapolation.

5 Discussion and Conclusions

The Lieb-Schultz-Mattis construction of gap-less excited states (1.4) in quasi one-dimensional spin-1/2 quantum spin systems demands translation invariance and short range couplings. To our knowledge systems which satisfy these conditions have no plateaus in their magnetisation curve for $M > 0$. In this paper we have studied the effect of a modulation of the couplings over $j = 1, 2, 3$ sites [cf. Eq. (1.6)] on the magnetisation process.

According to the quantisation rule of Oshikawa, Yamanaka and Affleck, we expect plateaus if the wave number q of the modulation coincides with one of the momenta of the soft modes $q^{(k)} = k\pi(1 - 2M),\ k = 1, 2, \ldots$. We have found, that the modulation of the nearest neighbour coupling [with the operator $\bar{\mathbf{D}}_1(q)$] generates one plateau at $M = 1/2 - q/\pi$, i.e. if q coincides with the first soft mode $q^{(1)}(M)$.

For $q = \pi$, the modulation of the nearest neighbour coupling with the operator $\bar{\mathbf{D}}_1(\pi)$ leads to the well-known singlet-triplet gap, i.e. a plateau at $M = 0$ – which opens with the strength δ of the perturbation as $\delta^{2/3}$[21,7].

The modulation of the next-nearest-neighbour coupling with $\bar{\mathbf{D}}_2(\pi)$ does not affect substantially the magnetisation process if $\delta < 0.4$. There is neither a plateau at $M = 0$ nor at $M = 1/4$. For $\delta > 0.4$, however, a plateau opens rapidly at $M = 1/4$ and shrinks again for $\delta > 0.7$. We have found that this effect is correlated with a change in the quantum numbers of the ground state.

Spin ladders with l legs can be mapped on one dimensional systems with modulated short range couplings. Of course these mappings are not unique. There are many possibilities to put a ring with nearest neighbour couplings on a ladder in such a way, that each site is passed once. The links which do not lie on the ring, define further reaching and modulated couplings. However, these mappings become unique, if we postulate that the range of the couplings is minimal. This means for normal ladders with l-legs, that the corresponding 1D system only contains modulated nearest neighbour couplings $[\bar{\mathbf{D}}_1(q)]$ and (translation invariant) couplings over l lattice sites. Here magnetisation plateaus appear if the wave vectors q of the magnetisation plateaus meet the *first* soft mode. The situation is different if we map zig-zag ladders on quasi 1D systems. Modulations of the next-nearest-neighbour couplings $[\bar{\mathbf{D}}_2(q)]$ emerge, which generate magnetisation plateaus if the wave vector q of the modulation meets either the first or the *second* soft mode.

Finally, we studied the magnetisation process of three leg zig-zag ladders with various boundary-conditions along the rungs. The boundary-conditions change the weight of the terms which modulate the couplings over one, two and three lattice spacings in the 1D Hamiltonian. This again affects the formation of plateaus at $M = 1/6$ and $M = 1/3$, respectively.

References

1. M. Oshikawa, M. Yamanaka, and I. Affleck, Phys. Rev. Lett. **78**, 1984 (1997).
2. K. Hida, J. Phys. Soc. Jpn. **63**, 2359 (1994).
3. K. Totsuka, Phys. Rev. B **57**, 3454 (1998).
4. D. C. Cabra, A. Honecker, and P. Pujol, Phys. Rev. Lett. **79**, 5126 (1997).
5. T. Tonegawa, T. Nishida, and M. Kaburagi, Physica B **246**, 368 (1998).
6. D. C. Cabra, A. Honecker, and P. Pujol, Phys. Rev. B **58**, 6241 (1998).
7. A. Fledderjohann, M. Karbach, and K.-H. Mütter, Euro. Phys. J. B **5**, 487 (1998).
8. D. C. Cabra, and M. D. Grynberg, Phys. Rev. B **59**, 119 (1999).
9. A. Fledderjohann, M. Karbach, and K.-H. Mütter, Euro. Phys. J. B **7**, 225 (1999).
10. A. Fledderjohann *et al.*, Phys. Rev. B **59**, 991 (1999).
11. E. Lieb, T. Schulz, and D. Mattis, Ann. Phys. **16**, 407 (1961).
12. I. Affleck and E. Lieb, Lett. Math. Phys. **12**, 57 (1986).
13. D. C. Cabra, A. Honecker, and P. Pujol, Euro. Phys. J. B **13**, 55 (2000).
14. C. N. Yang and C. P. Yang, Phys. Rev. **150**, 321 (1966).
15. C. Waldtmann, U. Schollwöck, K. Maisinger, and H. U. Everts, preprint **??**, ?? (1999).
16. A. K. Kolezhuk, Phys. Rev. B **59**, 4181 (1999).
17. J. C. Bonner and M. E. Fisher, Phys. Rev. **135**, A640 (1964).
18. P. Azaria, P. Lecheminant and A. A. Nersesyan, Phys. Rev. B **58**, R8881 (1998)
19. E. Lieb and D. Mattis, J. Math. Phys. **3**, 749 (1962).
20. C. Gerhardt, K.-H. Mütter, and H. Kröger, Phys. Rev. B **57**, 11504 (1998).
21. M. C. Cross and D. S. Fisher, Phys. Rev. B **19**, 401 (1979).